Performance Evaluation of Experimental 50-Mb/s Diffuse Infrared Wireless Link Using On–Off Keying with Decision-Feedback Equalization

Gene W. Marsh, *Member, IEEE*, and Joseph M. Kahn, *Member, IEEE*

Abstract—**We report an experimental nondirected optical link for short-range, indoor data transmission at 50 Mb/s. The system uses on–off keying (OOK) and achieves low bit-error rates (BER's) in the presence of intersymbol interference, background light noise, and shadowing, with a range of 2.9 m in a skylit room. The transmitter produces an eye-safe Lambertian pattern at 806 nm with an average power of 474 mW. The receiver utilizes a hemispherical concentrator with a hemispherical bandpass optical filter, a 1-cm^2 silicon p-i-n photodiode, and a high-impedance hybrid preamplifier to achieve a high signal-to-noise ratio (SNR). A high-pass filter is used to mitigate fluorescent light noise, with quantized feedback removing the resulting baseline wander. A decision-feedback equalizer provides resistance to intersymbol interference due to multipath. The system and its components are characterized, and compared to theory. We observe that decision-feedback equalization yields a reduction of multipath power penalties that is in good agreement with theory.**

Index Terms— **Infrared, wireless communications, local area networks.**

I. Introduction

INFRARED systems using direct detection provide significant advantages over radio systems for short-range, high-speed communication [1]–[3]. The available bandwidth is plentiful and unregulated, making it possible to establish links at very high bit rates. Since infrared radiation is blocked by walls and other opaque barriers, there is no interference between cells in different rooms, and links may easily be secured. Furthermore, because the square-law photodetector used in a direct-detection system is many times larger than the wavelength of the light, multipath propagation does not produce fading in a direct-detection system [4].

There are many configurations possible for indoor wireless infrared links. The transmitter and/or receiver may have a narrow field of view or a wide field of view, producing a directed or a nondirected system. Systems may also be classified as line-of-sight (LOS) or nonline-of-sight (non-LOS) depending on whether there is a direct path between transmitter and receiver. BT Laboratories has demonstrated a 155 Mb/s directed, LOS system using on-off keying (OOK) [5]. JOLT has produced a similar system that operates at 125 Mb/s [6]. IBM [7] and Photonics [8] have produced nondirected, non-LOS designs that allow *ad hoc*, peer-to-peer communication links between notebook computers using 16-pulse-position modulation (PPM). These systems achieve data rates of up to 1 Mb/s within a 10 m × 10 m room. Spectrix [9] offers a system that provides 4 Mb/s over a 15 m range using OOK. Each of these systems uses infrared light emitting diodes (LED's) as its light source.

We have chosen to study nondirected, non-LOS, or diffuse, links because they combine ease of use with robustness against shadowing [4]. In order to increase the bit rate of diffuse systems, several impediments must be overcome. As mentioned above, multipath propagation does not produce fading in infrared systems using direct detection. However, it does lead to distortion that produces significant intersymbol interference (ISI) at symbol rates above 10 Mbaud [3], [4], [10]. Infrared links are also impaired by noise due to background illumination. This comes in two forms. Sunlight, skylight, and incandescent lights represent sources whose intensity varies slowly with time. Such ambient light sources produce shot noise at the receiver. Because of the high level of steady illumination normally encountered, this can be modeled as a stationary, Gaussian, white noise with a power spectral density proportional to the total detected optical power. On the other hand, fluorescent lights flicker in a nearly deterministic, periodic fashion at the lamp drive frequency. This drive frequency may be that of the ac power lines (50 or 60 Hz) or, in the case of lamps driven by electronic ballasts, may be as high as tens of kilohertz. The resulting near-dc interference contains significant content at harmonics of the drive frequency, and thus may be detectable up to several hundred kHz [1], [3]. When the ambient illumination is sufficiently weak, the signal-to-noise ratio (SNR) of direct-detection links is limited by thermal noise of the receiver front-end preamplifier.

Previously, we reported a 50-Mb/s diffuse infrared system using baseband OOK [11]. The system was briefly described, and the basic performance of the system was characterized. In the current work, we characterize this system and its components in detail, comparing measured characteristics to

Paper approved by R. A. Valenzuela, the Editor for Transmission Systems of the IEEE Communications Society. Manuscript received September 15, 1995. This work has been supported by IBM, the California MICRO Program, an IBM Fellowship, and ARPA Contract J-FBI-92-150. This paper was presented in part at PIMRC'94, Hague, The Netherlands, September 1994.

G. W. Marsh is with Qualcomm, Inc., San Diego, CA 92121 USA (email: gwm@qualcomm.com).

J. M. Kahn is with the Department of Electrical Engineering and Computer Sciences, University of California, Berkeley, CA 94720-1772 USA (email: jmk@eecs.berkeley.edu).

Publisher Item Identifier S 0090-6778(96)08682-5.

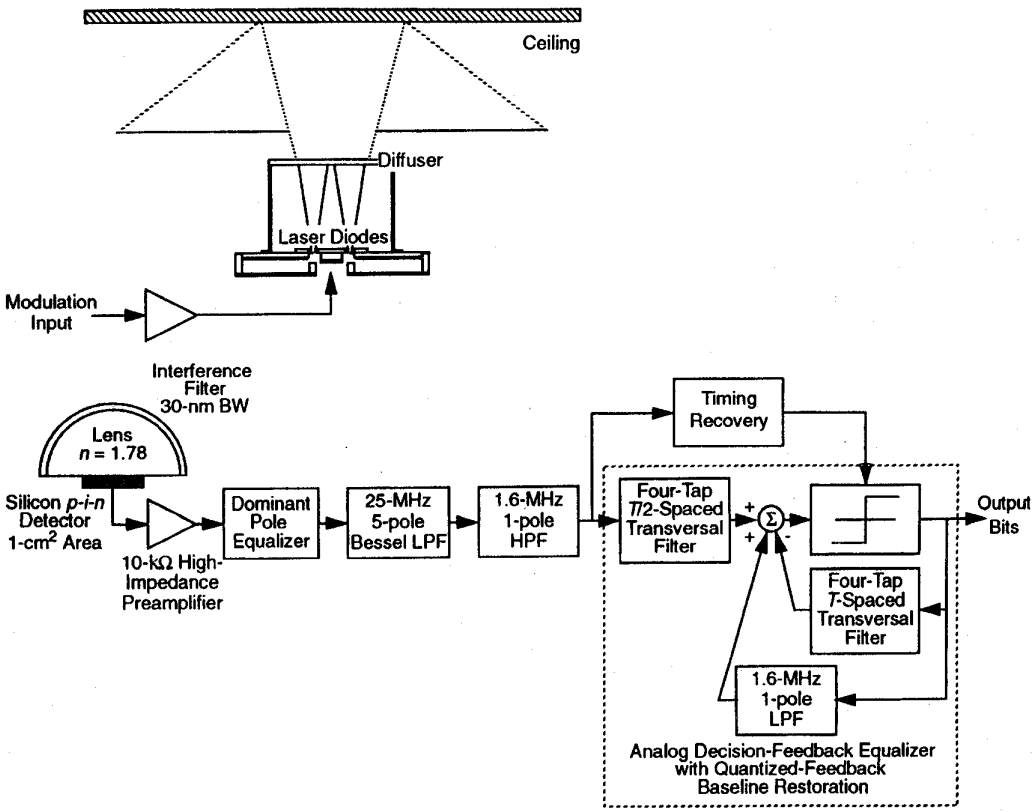

Fig. 1. System block diagram. The 806-nm transmitter emits an eye-safe, Lambertian pattern with order 1.85 at an average output power of 474 mW when modulated by OOK data. The receiver optics consist of a narrow-band, hemispherical optical filter bonded to the surface of a glass hemisphere. A 1-cm^2 silicon p-i-n photodiode drives a hybrid high-impedance amplifier followed by a 25-MHz low-pass filter. A high-pass filter reduces the impact of fluorescent light, and quantized feedback is used to remove the resulting baseline wander. A decision-feedback equalizer reduces the effect of ISI due to multipath.

the predictions of theory. This system uses a large-area, wide-field-of-view (FOV), narrow-band optical receiver to provide a high SNR in the presence of intense ambient illumination. A high-pass filter reduces the impact of fluorescent lights, with quantized feedback (QF) used to remove the resulting baseline wander [12]. A decision-feedback equalizer (DFE) mitigates ISI due to multipath.

II. System Design and Component Characterization

The block diagram of the system is shown in Fig. 1.

A. Transmitter

The light source for the transmitter is provided by eight Sony SLD302V-25 laser diodes (LD's), each of which has a nominal output power of 200 mW. The optical spectrum of the transmitter is shown in Fig. 2(a). The source output is centered at 806 nm, and has a width of 5.6 nm measured at −10 dBc, caused by emission into multiple longitudinal modes and by variations among device emission wavelength.

At the transmitter, the input electrical signal is used to drive eight amplifiers, and the output of each amplifier is combined with a dc bias current at each LD using a simple bias-tee network. The use of multiple LD's enables us to produce a source with a high peak transmit power, while using relatively modest driving amplifiers. The transmitter is flexible enough to support any intensity-modulation scheme. This system uses OOK, a modulation technique that represents a good compromise between power efficiency and bandwidth efficiency [2]. The use of OOK also enables us to mitigate multipath ISI through the use of a relatively simple DFE.

The light emitted from the LD's is passed through a 3-mm-thick piece of translucent white plexiglas. The net transmission of the plexiglas is 65%. The result is a source with an average power of 474 mW when transmitting OOK data. Fig. 2(b) shows the measured angular irradiance of the source when it transmits a steady output power of 340 mW. For comparison, Fig. 2(b) also displays the angular irradiance of a generalized point Lambertian source with order 1.85 having the same total power. The angular irradiance of this generalized point Lambertian source of order n is given by

$$\frac{dP}{d\Omega} = \frac{n+1}{2\pi} P_s \cos^n \theta \tag{1}$$

where P_s is the total source power and dP is the power radiated into the solid-angle element $d\Omega$ at an angle θ with respect to the source surface normal [1]. Examination of Fig. 2(b) shows that our source is well-approximated by the generalized Lambertian. Since the LD's illuminate an extended area of the plexiglas diffuser, the peak radiance of the source is 97 W/m^2-sr. This is well below the 121 W/m^2-sr allowable

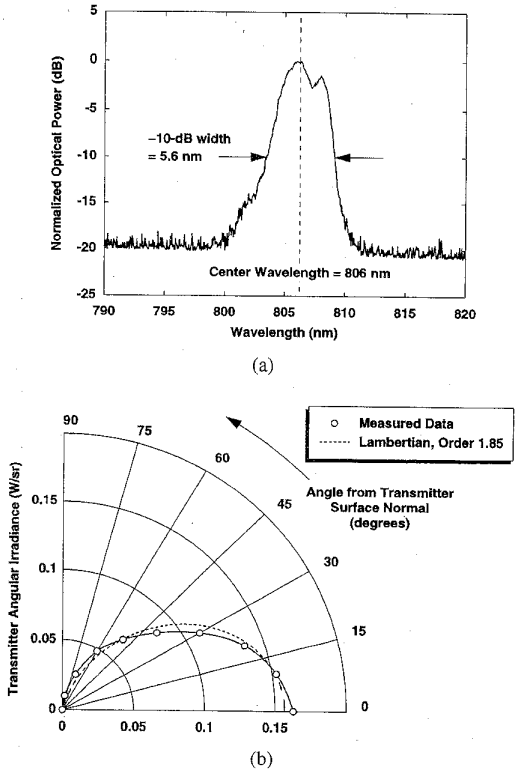

Fig. 2. Transmitter characterization. (a) Optical spectrum of transmitter output. The transmitter contains eight Sony SLD-302V multiple-longitudinal-mode laser diodes. (b) Angular irradiance of transmitter when operated at a constant output power of 340 mW. Also shown is the angular irradiance of a Lambertian source with order 1.85 having the same total power.

exposure limit for continuous viewing that is permitted under IEC-825-1 regulations [13].

During normal operation, the transmitter is placed near the center of the room and pointed upwards, illuminating a large area of the ceiling. This creates an extended source that can be "seen" from anywhere in the room, yielding robustness against shadowing of the receiver [4]. We refer to this as a diffuse transmitter configuration [2], [3].

B. Receiver

Light enters the receiver through a glass hemisphere, which serves as an optical concentrator that increases the effective light-collection area of the photodiode. The hemisphere has a refractive index of 1.78 and a radius of 2 cm. It is bonded to a photodiode using an index-matching compound having an index of 1.68. The photodiode is itself coated with a 153-nm thick, SiO antireflection (A/R) coating matched to the index of the lens. A hemispherical optical filter is used to reduce the effect of background light [2], [3]. The optical filter consists of three sections: a 22-layer short-pass filter, a 29-layer bandpass filter, and a 53-layer long-pass filter. This filter was fabricated on two pieces of 1-mm thick Kapton, which were epoxied together and then glued to the glass hemisphere. The final result has a center wavelength of 815 nm, a bandwidth of 30 nm, and a peak transmission of 68%. One of the properties of dielectric filters is that the filter passband shifts toward shorter wavelengths as the angle of incidence increases. Ray tracing indicates that any light rays that pass through the filter and eventually reach the photodiode will strike the filter at angles of incidence (with respect to the filter surface normal) between 0–30°. The filter bandwidth and center wavelength have been chosen so that the signal wavelength lies on the short-wavelength edge of the bandpass for an angle of incidence of 0° and on the long-wavelength edge of the bandpass when the angle of incidence is 30°. This design procedure insures that the received signal passes through the filter with little attenuation, while essentially minimizing the filter bandwidth, and thus the received ambient noise [2], [3], [14].

In computing the performance expected of our receiver optical system, we assume that a plane wave is incident upon the receiver at an angle ψ with respect to the photodiode surface normal. A ray that is eventually detected will strike the hemispherical filter at an incidence angle θ_0, strike the index-matching compound at an angle θ_1, and then strike the photodiode A/R-coating at an angle of θ_2. Let $S(\psi)$ be the set of all points on the surface of the lens for which light from a ray entering the system at angle ψ strikes the surface of the photodiode. Let $\hat{I}$ be the incidence vector for such a ray. Then, the effective light-collection area [2], [14] of the photodiode as a function of ψ is given by

$$A_{eff}(\psi) = -\int_{S(\psi)} T_f(\theta_0) T_g(\theta_1) T_p(\theta_2)\,(\hat{I}\cdot d\hat{S}) \qquad (2)$$

where T_f is the transmittance of the optical filter at the signal wavelength, T_g is the transmittance through the index-matching compound, and T_p is the transmittance of the photodiode A/R coating. The gain in effective area relative to an ideal, perfectly absorbing Lambertian detector is given by

$$G(\psi) = \frac{A_{eff}(\psi)}{A_{det}\cos\psi} \qquad (3)$$

where $A_{\rm det}$ is the area of the photodiode [2], [14]. This gain translates directly into an increase in received optical power. We compute (2) and (3) using numerical ray-tracing techniques.

Fig. 3(a) displays the measured effective area of our receiver optical system. Also shown in Fig. 3(a) is the effective area measured when the hemispherical filter-hemisphere combination have been replaced by a simple hemispherical lens having an A/R coating. For reference, the effective area of an ideal, 1-cm^2 Lambertian detector is also shown. The A/R-coated hemisphere produces a nearly omnidirectional receiver whose apparent area is in good accordance with theory. The measured effective area of the lens-filter combination is somewhat smaller than predicted by theory; the observed discrepancy may be explained, at least in part, by scattering losses within the optical system, and by our neglect of the nonzero source spectral width in computing the filter transmission T_f in the theoretical evaluation of the effective area (2). The lens-filter combination achieves a field of view (FOV) of 65° (half-angle), which we define as the value of ψ at which the effective area becomes half that for $\psi = 0°$.

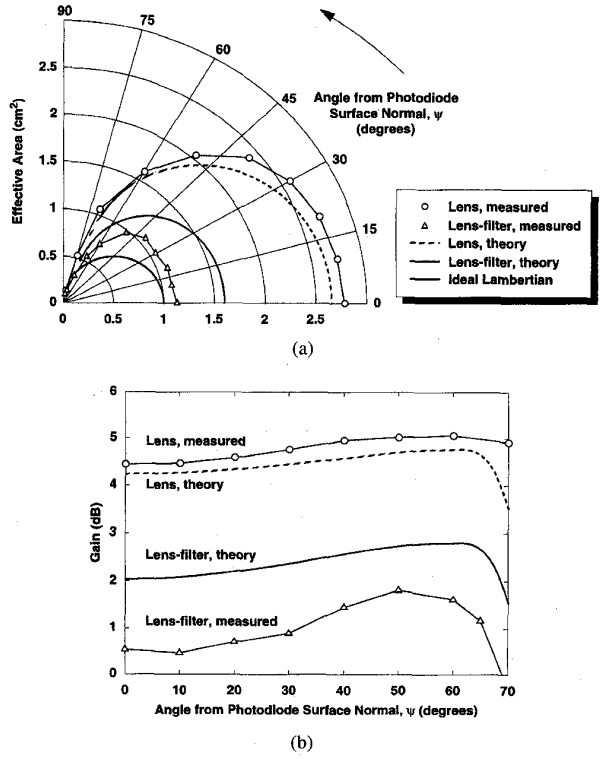

Fig. 3. Effective light-collection area and optical gain for signal light incident on receiver at angle ψ with respect to photodiode surface normal. (a) Effective area of hemispherical lens, hemispherical filter-lens combination, and ideal Lambertian detector. (b) Optical gain of hemispherical lens and lens-filter combination, which is ratio of respective effective areas to area of Lambertian detector.

In Fig. 3(b), we compare the optical gain of the A/R-coated hemisphere and the filter-hemisphere combination to the predictions of theory. The A/R-coated hemisphere attains an overall optical gain of 5.05 dB, which is very close to the theoretical maximum of $\log_{10}(n^2) = 5.01$ dB [2]. The optical system consisting of the glass hemisphere and filter has a peak gain of 1.8 dB, which is about 1.0 dB below the value predicted by theory. Our receiver's simultaneous achievement of net optical gain, narrow bandwidth, and wide FOV is a direct consequence of the use of the hemispherical optical filter [2], [14].

After passing through the optical filter and concentrator, the light strikes a 1-cm^2 silicon positive-intrinsic-negative (p-i-n) photodiode (EG&G YAG-444), which is n-illuminated and has a thickness of 320 μm, a shunt capacitance of 35 pF, and a series resistance of 5 Ω. The resulting photocurrent is amplified by a hybrid, high-impedance amplifier. The amplifier employs a 10-kΩ load resistance, followed by an Oki KGF1850 high electron mobility transistor (HEMT) in a common-source configuration. When biased at $I_{DS} = 30$ mA and $V_{DS} = 2$ V, the HEMT has an f_T of 44 GHz, a transconductance of 126 mS, and a "corner frequency" for $1/f$ noise of 258 MHz (this is the frequency below which the power spectral density of the $1/f$ component of the channel noise exceeds that of the white component).

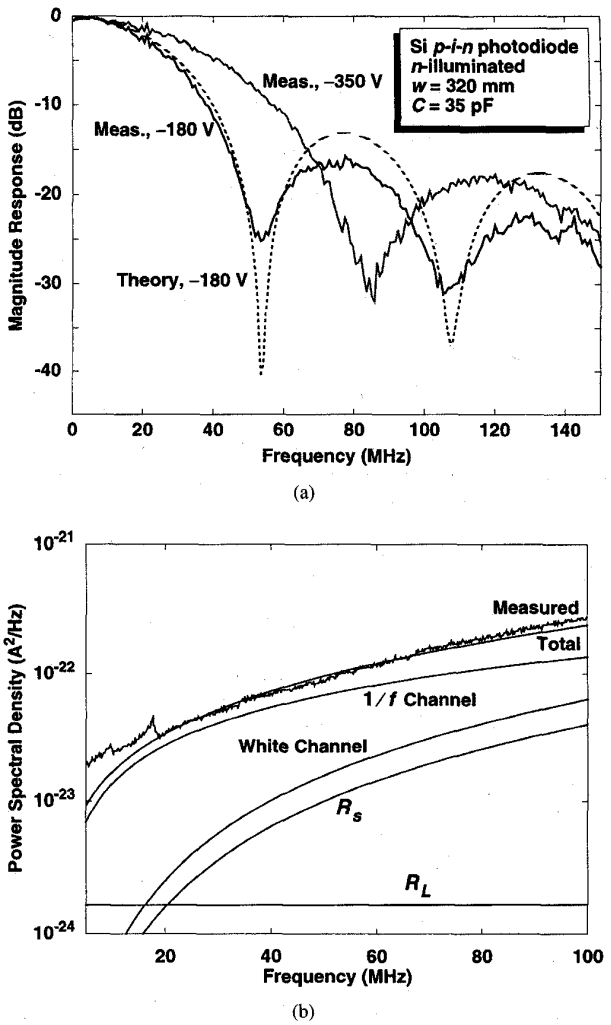

Fig. 4. Receiver preamplifier characterization. (a) Measured receiver magnitude response. The frequency response is dominated by transit-time limitations in the n-illuminated silicon p-i-n photodiode, which is seen in comparison of measurements at biases of -180 V and -350 V. The theoretical response at -180 V is also shown. (b) Preamplifier input-referred noise power spectral densities, measured and theoretical. The theoretical dominant noise sources are also shown individually. These are noises arising from the white channel noise, the $1/f$ channel noise, the photodiode series resistance (labeled R_s), and the load resistor (labeled R_L). The equivalent input noise current density (one-sided) is 5.73 pA/$\sqrt{\text{Hz}}$, averaged over the bandwidth of the receiver filter.

The measured receiver magnitude response is displayed in Fig. 4(a). The amplifier response is dominated by the single pole at 455 kHz formed by the load resistance and the photodiode capacitance. A passive R-C circuit compensates this pole. However, at the signal wavelength of 806 nm, most of the electron-hole pairs are generated within tens of microns of the illuminated n-type photodiode contact region. Under reverse bias, the electrons travel back to the n-contact, but the holes, whose velocity is about three times smaller, must traverse the much longer distance to the p-contact. This leads to a transit-time bandwidth limitation. Under a reverse bias of -180 V, the 3-dB bandwidth is only 23.4 MHz, while a bias of -350 V increases the bandwidth to 33 MHz. Fig. 4(a) also

shows the theoretical transit-time-limited detector magnitude response [15] for a bias of -180 V, which is in good agreement with our experimental observations. For all system measurements reported in this paper, the detector bias was set at -180 V, and the limited receiver bandwidth introduced some ISI that must be taken into account in predicting system performance.

The measured and theoretical input-referred noise power spectral densities [16] of the preamplifier are shown in Fig. 4(b). The dominant noise sources are also shown individually. These are the noises arising from the white and $1/f$ components of the HEMT channel noise, from the series resistance of the photodiode, and from the load resistor. It can easily be seen that the receiver input-referred noise is dominated by the $1/f$ channel noise. The equivalent input noise current density (one-sided) is 5.73 pA/$\sqrt{\text{Hz}}$, averaged over the bandwidth of the 25-MHz, five-pole Bessel receiver filter. This is equivalent to the shot noise from an input DC photocurrent of 142 μA, after taking into consideration the photodiode transit-time limitations.

A 25-MHz, five-pole, Bessel, low-pass filter is employed to limit shot noise and receiver thermal noise. In addition, to reduce the impact of near-dc fluorescent-light interference, we employ a single-pole high-pass filter having a 3-dB cut-on frequency of 1.6 MHz. This introduces baseline wander into the received signal. By passing the decision-circuit output through a single-pole low-pass filter that has a 3-dB cutoff of 1.6 MHz, the baseline wander can be predicted and, thus, removed from the system. This technique is known as quantized feedback (QF) [12].

A DFE reduces the impact of ISI arising from multipath distortion. The forward filter consists of four taps that are spaced one-half baud apart, and the reverse filter consists of four taps that are spaced one baud apart. These filters are constructed using analog tapped delay lines and manually controlled tap gains.

Timing recovery is performed using a second-order phase locked loop with a damping factor of 0.707 and a natural frequency of 30 krad/s.

III. System Characterization

We have characterized the system performance in two ways. First, we evaluated the performance in the absence of ambient lighting. These measurements tested our ability to predict the system performance with and without equalization, and allowed us to study the effect of shadowing. Second, we tested the system under different lighting conditions, to quantify the impact of ambient light noise.

A. Performance in Absence of Ambient Lighting

In order to test the efficacy of the DFE, we operated the system in four different rooms. The dimensions of the rooms used, and the positions of the transmitter and receiver, are illustrated in Fig. 5. All of the rooms had off-white-colored walls and ceilings. Within each room, measurements were taken at five different transmission distances, including an unequalized bit-error rate (BER) curve, an equalized BER curve, and the link frequency response. These frequency responses include not only the multipath channel, but also the characteristics of both the transmitter and the receiver preamplifier. All BER measurements were performed using a $2^7 - 1$ pseudo-random bit sequence. QF was not used during these measurements, and the 1.6-MHz high-pass filter was replaced by a 159-kHz high pass filter. At one transmission distance in each room, the same data set was recorded, but with a 1.74-m-high human silhouette placed 30.5 cm from the receiver, along a line between transmitter and receiver, so as to simulate shadowing. At each transmission distance, an optical power meter having a FOV equal to that of the receiver was used to measure the average received power.

Because our DFE implementation prevented the use of an automatic adaptation algorithm, adjustment of the DFE tap weights was the most complicated part of the measurement process. The taps were generally adjusted in an empirically determined sequence, starting with the taps of the forward filter and working through the taps of the reverse filter. An oscilloscope was used to monitor the eye pattern at the decision-circuit input, and a device was attached to the BER testset that yielded an audible indication of the BER. The operator monitored the eye pattern, and adjusted the taps to minimize the BER.

Fig. 6(a) displays the variation of optical path loss with distance in each room, as determined from the link frequency responses. We define the path loss to be the ratio of the transmitted power to the power received by a detector having an effective area of 1 cm^2 and a FOV of 65°. For example, when the transmitted power is 1 W, a path loss of 60 dB corresponds to a received irradiance of -30 dBm/cm^2. It can be seen in Fig. 6(a) that within any particular room, the path loss increases monotonically with increasing transmission distance. The path loss is observed to increase as the room size increases. The effect of shadowing on path loss depends on the ceiling height. In rooms having relatively low ceilings, shadowing increases the path loss by 3.0–3.6 dB. In Room C, where the ceiling is considerably higher, and the shadowing data were taken at a smaller horizontal separation, the increase in path loss is only 1.1 dB.

One measure of the severity of a channel's multipath distortion is its root-mean-square (rms) delay spread. This is the square root of the second central moment of the magnitude squared of the impulse response of the channel, where the impulse response has been normalized to unit energy [4]. Fig. 6(b) displays the dependence of delay spread on transmission distance within each room. The delay spread generally exhibits a slight increase with increasing distance from the source. The delay spread (and, more generally, the channel impulse response) tends to have a stronger dependence upon the dimensions and reflectivities of the room than upon the transmission distance. Accordingly, we observed that it was often possible to move the receiver a distance up to 0.25 m before DFE readjustment became necessary. The delay-spread

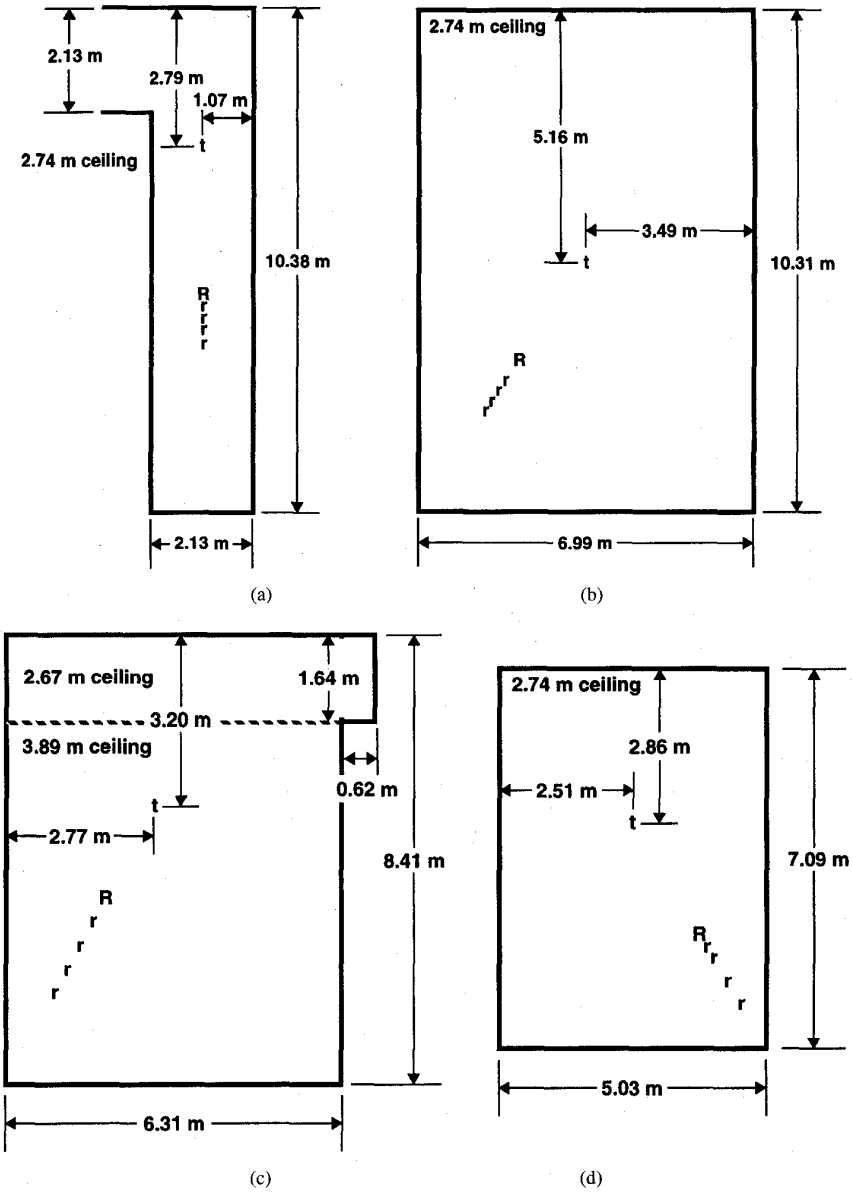

Fig. 5. Schematic representation of the rooms used for system testing. (a) Room A, (b) Room B, (c) Room C, and (d) Room D. The "t" represents the position of the transmitter. An "r" indicates a position at which measurements were taken without shadowing of the receiver, while "R" indicates a position at which a shadowed measurement was taken.

data also indicates that shadowing results in a broadening of the impulse response.

Fig. 7(a) presents the equalized receiver sensitivity as a function of the rms delay spread; the sensitivity is defined as the received irradiance at which 10^{-9} BER was achieved. There is a clear tendency for the equalized power requirement to increase with increasing delay spread, a relationship that has been observed in theoretical performance predictions [4]. Because of the relationship between delay spread and distance, we also observe a slight tendency for the required power to increase as the transmission distance is increased.

For every set of data taken, a BER was chosen at which to compare the performance of the system with and without equalization. These BER's ranged from 5×10^{-2} to 10^{-7}. Once that BER was chosen, the theoretical penalties with and without equalization at that BER were computed using the measured channel impulse response. The unequalized penalties were computed using a moment generating function technique [17]; when this failed to converge rapidly, an enumeration technique was substituted [2]. Equalized penalties were computed by assuming that the BER was related to the ratio of the signal level to the mean-squared error at the decision-circuit input, treating the equalizer as a minimum-mean-squared-error equalizer [18]. Fig. 7(b) shows the theoretical DFE gains plotted against the measured DFE gains. The data points lie scattered close to a line of unit slope, indicating good agreement between experiment and theory. The variance of the data points increases with increasing gain. This is largely

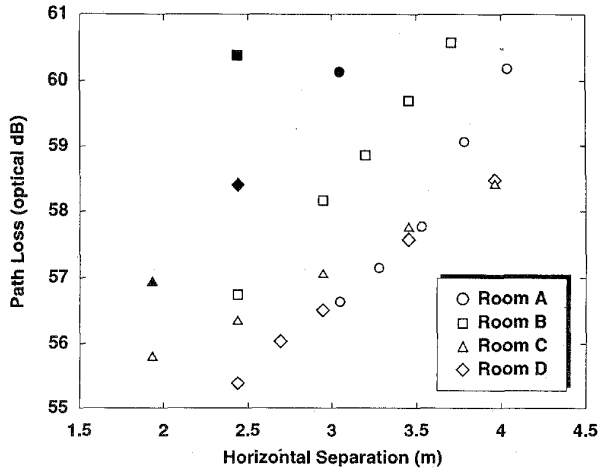

(a)

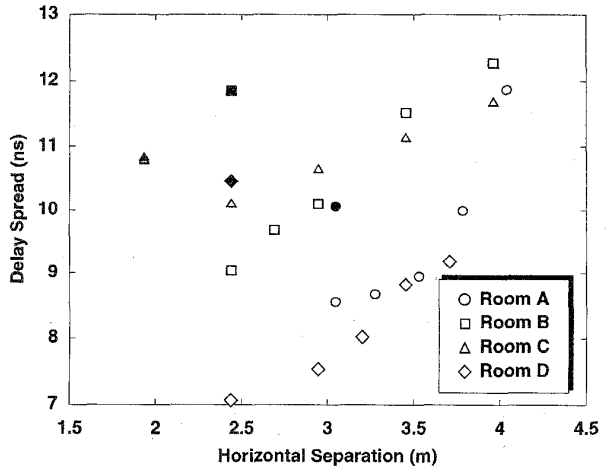

(b)

Fig. 6. (a) Optical path loss as a function of horizontal separation. All path losses have been determined from the link frequency responses. (b) Root-mean-square delay spread versus horizontal separation. There is a slight increase in delay spread with increasing distance, but the room parameters have a greater impact. Hollow symbols represented unshadowed configurations, while solid black symbols represent shadowed configurations.

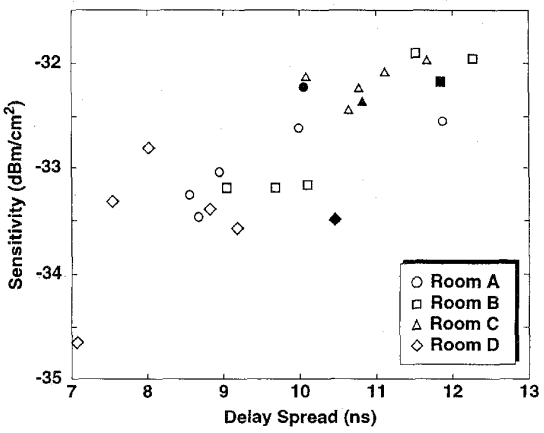

(a)

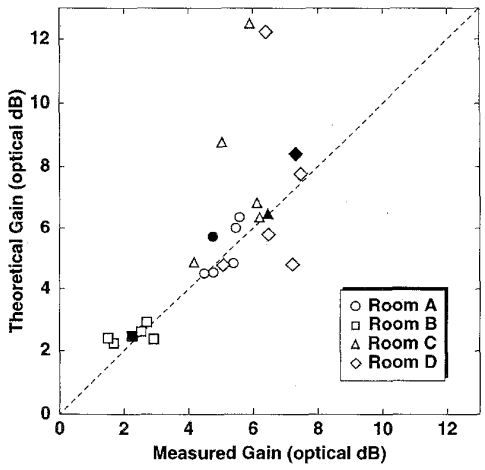

(b)

Fig. 7. Performance evaluation with ISI due to multipath. Hollow symbols represent unshadowed configurations, while solid black symbols represent shadowed configurations. (a) Equalized receiver sensitivity (at 10^{-9} BER) versus root-mean-square delay spread. Note that the required illumination tends to increase with increasing delay spread. (b) Gain in optical power efficiency due to decision-feedback equalization: comparison of theory and experiment. The data points lie along a line of unit slope, indicating good agreement between theory and experiment. The variance of the data points increases with increasing gain. Note that a 1-dB optical gain corresponds to a 2-dB gain in electrical signal-to-noise ratio.

due to uncertainty in the calculation of the unequalized penalty, which becomes more difficult to calculate precisely when ISI is severe.

It is worth noting that our experimental evidence suggests that all of the effects of shadowing (increased path loss and delay spread) can be overcome simply by increasing the transmitter power by approximately 3.5 dB.

B. Performance in the Presence of Ambient Lighting

As the interference from fluorescent lighting is primarily low-pass in nature, use of a high-pass filter combined with QF is employed to reduce the impact of fluorescent lights. The QF has an adjustable gain so that it can be matched to the signal amplitude at the decision-circuit input. This tap weight is adjusted to minimize the BER of the system. When combining QF with the DFE, the QF tap weight is adjusted first, then the DFE weights are adjusted. Fine tuning is done by alternately adjusting the QF tap weight and the DFE tap weights.

Fig. 8(a) illustrates the impact of various ambient light sources on the BER-versus-irradiance performance of the 50-Mb/s link. These data were recorded in Room C, which has windows facing south and west. During all measurements shown in Fig. 8(a), the transmitter and receiver were kept in the same locations, separated by a horizontal distance of 3.05 m, the receiver was unshadowed, and the DFE was used to counter ISI. Bright skylight, which induced a receiver photocurrent varying from 111–115 μA during the measurement, degraded performance by 1.5 dB at a BER of 10^{-9}. We note that this is approximately a 3-dB change in electrical SNR, which is consistent with the measured input-referred receiver

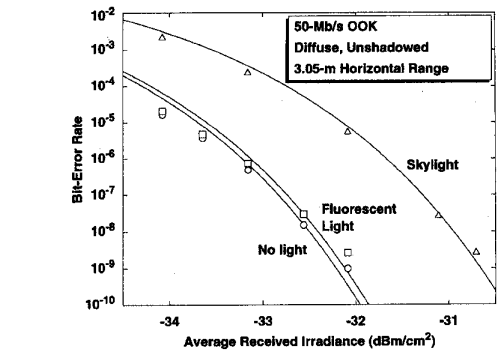

(a)

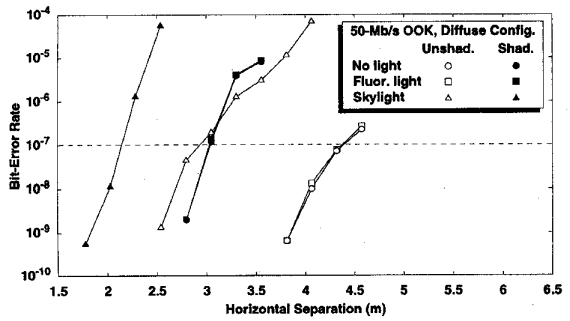

(b)

Fig. 8. Performance variation with background light. Data were taken in Room C, which has windows facing south and west. Three different light conditions were used: No background light, fluorescent light, and skylight. Decision-feedback equalization was employed in all cases. (a) Effect of background light on the bit-error-rate performance of the 50-Mb/s OOK system. Transmitter-receiver horizontal separation was fixed at 3.05 m. (b) BER versus horizontal transmitter-receiver separation for the 50-Mb/s OOK system, illustrating the effect of shadowing and background illumination. Shadowing was provided by 1.74-m-high human silhouette placed 30.5 cm from the receiver, along the line joining the transmitter and receiver. Note that the system has a range of 2.9 m in skylight without shadowing (at 10^{-7} BER).

noise. A penalty of only 0.1 dB was induced by the emission from fluorescent lamps driven by 22-kHz solid-state ballasts.

The variation of link BER with horizontal transmission distance with full transmitter power, under various lighting conditions, is shown in Fig. 8(b). These data were recorded in Room C. During all measurements, the DFE was employed. In the absence of shadowing, with no illumination the link achieved a range of 4.4 m (defined as the maximum horizontal separation at which 10^{-7} BER could be achieved). With shadowing, the link range was reduced to 3.0 m without ambient lighting. These ranges remained unchanged in the presence of fluorescent lighting. The range was also measured with bright skylight. Without shadowing, the skylight introduced a receiver photocurrent of 165 to 335 μA. The skylight increased as the distance to the source decreased, primarily due to changes in the distance between the receiver and the windows, accounting for the kink in the associated curve. Skylight reduced the link range to 2.9 m. In testing the system with bright skylight and shadowing, the background light induced a photocurrent ranging from 160–236 μA. Under these conditions, the range achieved was about 2.1 m.

IV. Conclusion

We have demonstrated transmission of 50-Mb/s data at low BER using diffuse infrared radiation. OOK modulation with a DFE is effective in countering multipath-induced ISI. Through use of a hemispherical optical bandpass filter and high-index, hemispherical concentrator, the receiver achieves immunity to ambient infrared radiation, while maintaining a wide FOV. The impact of fluorescent lighting has been mitigated by means of high-pass filtering and QF baseline restoration. In a brightly skylit room, an unshadowed link achieves a range of 2.9 m. The effects of receiver shadowing could be overcome if we could increase the transmitter power by approximately 3.5 dB.

Study of this data suggests a number of improvements that might be made to this system. The use of a p-illuminated photodiode would significantly increase the receiver bandwidth, allowing us to transmit at higher bit rates. The thermal noise of our receiver is dominated by the contribution from the $1/f$ noise of the HEMT channel. Use of a transistor having reduced $1/f$ noise, while maintaining similarly low input capacitance and high transconductance, could reduce the receiver thermal noise substantially. This would improve the receiver sensitivity, particularly in the absence of skylight-induced shot noise. Finally, it should be possible to decrease the transmission losses of the optical filter and concentrator, which would translate directly to an improvement in receiver sensitivity.

Acknowledgment

The authors would like to thank Sony Corporation for their contribution of the laser diodes, M.-H. Kiang for wire-bonding the receiver, J. Potter of Barr Associates whose expertise made it possible to produce a hemispherical optical filter, and J. Carruthers and M. Audeh for helpful discussions about multipath channels.

References

[1] F. R. Gfeller and U. H. Bapst, "Wireless in-house data communication via diffuse infrared radiation," *Proc. IEEE,* vol. 67, no. 11, pp. 1474–1486, Nov. 1979.
[2] J. R. Barry, *Wireless Infrared Communications.* Boston: Kluwer, 1994.
[3] J. M. Kahn, J. R. Barry, M. D. Audeh, J. B. Carruthers, W. J. Krause, and G. W. Marsh, "Non-directed infrared links for high-capacity wireless LAN's," *IEEE Personal Commun. Mag.,* vol. 1, no. 2, pp. 12–25, May 1994.
[4] J. M. Kahn, W. J. Krause, and J. B. Carruthers, "Experimental characterization of nondirected indoor infrared channels," *IEEE Trans. Commun.,* vol. 43, no. 2–4, pp. 1613–1623, Feb./Mar./Apr. 1995.
[5] M. J. McCullagh and D. R. Wisely, "155 Mbit/s optical wireless link using a bootstrapped silicon APD receiver," *Elec. Lett.,* vol. 30, no. 5, pp. 430–432, Mar. 3, 1994.
[6] Jerusalem Optical Link Technologies (JOLT), Ltd., Jerusalem, Israel.
[7] International Business Machines Corporation, Armonk, NY.
[8] Photonics Corporation, San Jose, CA.
[9] Spectrix Corporation, Evanston, IL.
[10] J. R. Barry, J. M. Kahn, W. J. Krause, E. A. Lee, and D. G. Messerschmitt, "Simulation of multipath impulse response for wireless optical channels," *IEEE J. Select. Areas Commun.,* vol. 11, no. 3, pp. 367–379, Apr. 1993.
[11] G. W. Marsh and J. M. Kahn, "50-Mb/s diffuse infrared free-space link using on-off keying with decision feedback equalization," *IEEE Photonics Tech. Lett.,* vol. 6, no. 10, pp. 1268–1270, Oct. 1994.

[12] F. D. Waldhauer, "Quantized feedback in an experimental 280-Mb/s digital repeater for coaxial transmission," *IEEE Trans. Commun.,* vol. COM-22, pp. 1–5, Jan. 1974.
[13] "CEI/IEC825-1: Safety of laser products," in *Int. Electrotechnical Commission,* 1993.
[14] J. R. Barry and J. M. Kahn, "Link design for nondirected wireless infrared communications," *Appl. Optics,* vol. 34, no. 19, pp. 3764–3776, July 1995.
[15] B. E. A. Saleh and M. C. Teich, *Fundamentals of Photonics.* New York: Wiley, 1991.
[16] S. D. Personick, "Receiver design for digital fiber optic communications systems, I and II," *Bell Sys. Tech. J.,* vol. 52, no. 6, pp. 843–886, July/Aug. 1973.
[17] J. B. Carruthers and J. M. Kahn, "Multiple-subcarrier modulation for nondirected wireless infrared communication," *IEEE J. Select. Areas Commun.,* submitted.
[18] E. A. Lee and D. G. Messerschmitt, *Digital Communications,* 2nd ed. Boston, MA: Kluwer, 1994.

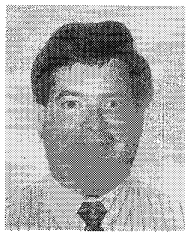

Gene W. Marsh (M'84) received the B.S. degree in computer science and electrical engineering from Rose-Hulman Institute of Technology, Terre Haute, IN, in 1981, the M.S. degree in electrical engineering from Stanford University, CA, in 1987, and the Ph.D. degree in electrical engineering from the University of California at Berkeley in 1995.

His Ph.D. dissertation was entitled "High-Speed Wireless Infrared Communication Links." He is currently employed as a systems engineer at Qualcomm, Incorporated in San Diego, CA.

Joseph M. Kahn, (M'87) for a photograph and biography, see this issue, p. 1443.